

# Spectral and energy efficiency trade-off in massive MIMO systems using multi-objective bat algorithm

Burak Kürşat Gül, Necmi Taşpınar<sup>1</sup>

The rise in the usage of wireless communication increases the cellular communication by the same rate. With the continuation of this situation, the density in data traffic has the potential to cause problems in the near future. Coping with spectral efficiency-energy efficiency trade-off using massive MIMO systems is considered to be a reasonable solution to this problem. In this paper, cellular communication simulations were performed in cases with different number of users, number of antennas and transmission power of massive MIMO systems and then non-dominated solutions are determined. Multi-objective bat algorithm has been used to make this process much shorter. At last stage, performance of this algorithm is compared with various intelligent optimization algorithms and with ideal non-dominated solutions. When the algorithms are compared with each other, it is seen that multi-objective bat algorithm has the best performance among them.

**Key words:** energy efficiency, spectral efficiency, massive MIMO, multi-objective bat algorithm

## 1 Introduction

Wireless communication technology has been adopted and appreciated to a level that it has become a daily need for people. Especially with the rise of widespread areas of use, there has been a desire to always stay online in every environment. This situation leads to an increase in data transfer using cellular communication, thus increasing the data traffic. In order to continue to meet the demands of the users, it is necessary to deal with the density of data traffic. This requires the area throughput (TR) to be increased considerably in the near future [1].

Nowadays increasing spectral efficiency SE is one of the actions that can be taken to increase the area throughput. Spectral efficiency (bit/s/Hz) is equivalent to the average number of bits for each complex-valued sample of information, in other words, the number of bits successfully transmitted in unit bandwidth. Spectral efficiency can be increased by factors such as increasing the number of users served in a cell and establishing a more reliable connection between the receiver and transmitter. While increasing spectral efficiency, factors such as using more antennas and increasing transmission power can increase the amount of energy consumed. Excessive increase in the level of energy consumed is an undesirable situation because it endangers natural resources and is costly. Therefore, while working on spectral efficiency, care is taken to ensure that the energy consumed is at reasonable levels and energy efficiency (EE) is also emphasized. Energy efficiency (bit/J) refers to the amount of bits successfully transmitted using unit energy [2].

## Related Works

Massive multi-input multi-output (massive MIMO) systems, which are a preferred method for increasing the number of user equipments (UEs) served among the cell, represent a successful technology for cellular communication. It is known that massive MIMO systems are successful to increase both spectral efficiency and energy efficiency [1]. Moreover, some studies are carried out on massive MIMO systems at different subjects in the literature [3–9]. In [3] the large uniform linear array was considered and a novel sectorization method with low complexity was proposed so it is seen that the sum-throughput could be greatly increased compared to the typical massive MIMO architecture. A hybrid wireless network model is used in [4], in which each base station is connected by a wired connection, and the outage capacity and ergodic capacity in this scenario have been investigated. In [5], massive MIMO systems including a hybrid data-and-energy access point and multiple single-antenna users have been researched for wireless-energy-transfer. In order to improve the performance of the systems, two techniques have been introduced in [6] that control the transmission power of users and reduce cellular-to-device to device and device to device-to-cellular interference. In [7], performance evaluations have been made in existing practical networks via performing massive MIMO multi-user space division multiplexing based on transmission mode by dividing the massive MIMO antenna into a virtual beam and fan section. A massive MIMO and interleave division multiple access (IDMA) communication system has been jointly proposed in [8], and the minimum mean square error based beamformer has been suggested for a

<sup>1</sup>Department of Electrical and Electronics Engineering, Erciyes University, Kayseri, Turkey, burak.gul@erciyes.edu.tr, taspinar@erciyes.edu.tr

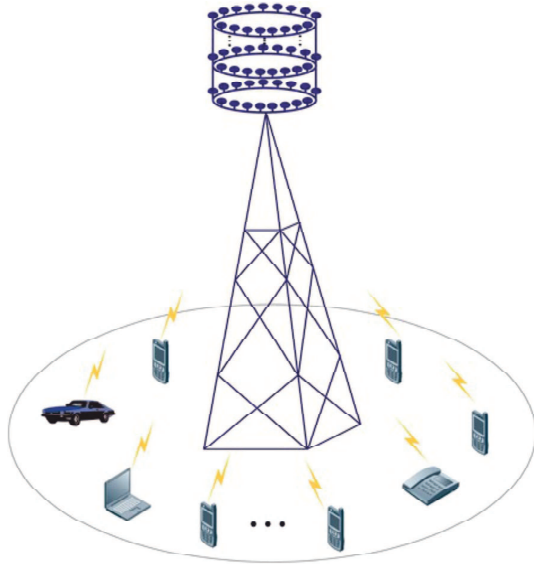


Fig. 1. Sample of massive MIMO cell [13]

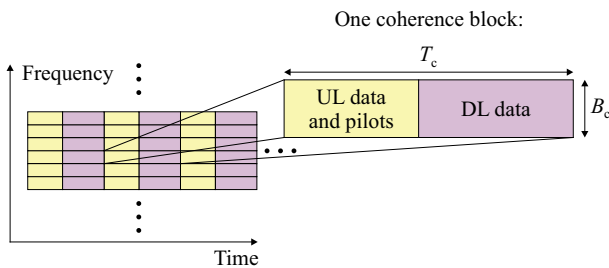


Fig. 2. TDD multicarrier modulation scheme [1]

massive MIMO-IDMA system under downlink communication constraints. In [9], in the cells using massive MIMO systems, the trade-off of spectral and energy efficiencies has been optimized with intelligent optimization algorithms and the effect of circuit powers has been investigated using different power sets.

In the literature, there are studies using intelligent optimization algorithms on SE-EE trade-off for massive MIMO systems [10, 11]. In [10] the effects of active antenna number values on SE-EE trade-off are examined, and it was focused on converting this trade-off from multi-objective optimization (MOO) problem to single-objective optimization (SOO) problem. Since MOO problems are highly complex in terms of discrete and continuous-time variables and they do not have solutions in closed form, it has been deemed appropriate to transform MOO problems into SOO problems. In the study, two new SOO methods have been developed using the simple and fast converging particle swarm optimization (PSO) method. The first of these is the weighted-sum PSO (WS-PSO) algorithm, in which PSO is combined with the weighted-sum technique, which is widely used in the conversion from MOO to SOO. The second algorithm is the normal-boundary-intersection (NBI-PSO) algorithm, which is a combination of the NBI technique

and PSO, which is more successful in converting from MOO to SOO. In [11] the effect of the number of antennas used and transmit power on the SE-EE trade-off is examined. In the study, the genetic algorithm (GA), which is known to perform well when discrete and continuous variables are used at the same time, is emphasized and a multi-purpose adaptive version of the genetic algorithm has been developed. The multi-objective adaptive genetic algorithm, developed on the basis that MOO-SOO transformation methods cannot work effectively on the entire Pareto curve, is a separate gene pool, unlike standard GA. This pool consists of SE-EE values that cannot be dominated by other SE-EE values. These elements that cannot be dominated are obtained by applying genetic processes on genes that can be dominated until the pool reaches a sufficient size. After the pool reaches a sufficient size, crossover and mutation stages are started. Finally, the results of the problem which is modelled as a mixed-integer-continuous-variable MOO problem have been researched.

#### Contributions of the paper

The main contributions of this paper are the following:

1. Multi-objective bat algorithm (MOBA), which we can describe as more modern than the algorithms used in the studies in the literature, is applied on SE-EE trade-off in massive MIMO systems for the first time.

2. The number of users, which directly affects the SE-EE trade-off, has been added to the decisive variables in the optimizations, so that the optimizations are performed with three independent variables,  $K$  – the number of users,  $M$  – the number of antennas and  $p$  – the transmission power. This process allows the evaluation of more different scenarios compared to the studies in the literature where only  $M$  and  $p$  are optimized, and increases the depth of optimizations.

## 2 System model

Having a large number of user equipment and active antenna in a cell is the most prominent feature of massive MIMO systems. In these systems,  $M > K$  and  $M \gg 1$  conditions are always tried to be met and provision of these conditions makes the cellular networks almost immune to fading and interference [12]. A sample of massive MIMO cell is shown in Fig. 1.

Time-division duplex (TDD) protocol is preferred for multicarrier modulation on a canonical massive MIMO network. Thanks to the use of this protocol, channel responses are reciprocal and so fewer pilot bits are required. In Fig. 2 TDD multicarrier modulation scheme of a canonical massive MIMO is shown, where  $T_c$  is coherence time and  $B_c$  is coherence bandwidth.

Each coherence block contains  $B_c T_c$  complex-valued samples. But the number of practically useful samples per coherence block can be smaller than  $B_c T_c$ . Because there may be situations that require symbol time such as the cyclic prefix in OFDM.

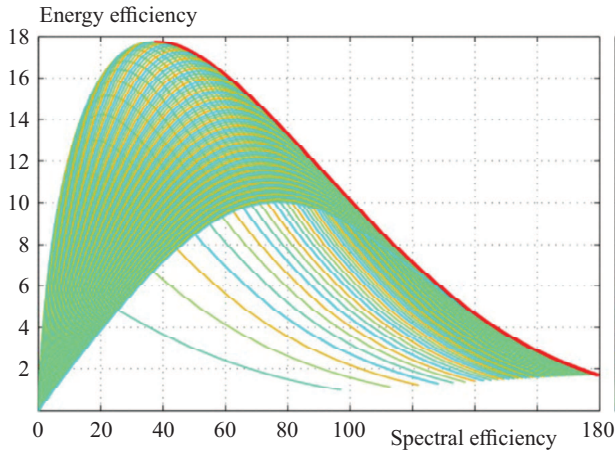


**Fig. 3.** SE-EE values in cases where various antenna numbers and transmission power are used [11]

---

```

Define the parameters of the algorithm
Initialize the population (bats) with random combinations of [K, M, p]
Calculate the fitness values (SE and EE) of all population
while (t < max number of iterations)
  Define the loudness (A) and the pulse emission rate (r) as in (1) and (2)
  for (j = 1 to size of population)
    Generate a new solution and update
    if (rand > r)
      Random walk around the best solution
    end if
    Calculate fitness values of new bat
    if (new bat dominates the old one or rand < A)
      Accept new solution
    end if
  end for
  Rank the bats and find the current best bat
end while
Save the non-dominated solutions

```

---

**Fig. 4.** Pseudo code of MOBA applied to SE-EE trade-off problem

As a solution for data traffic and energy problem, increasing SE and EE values can be considered by using massive MIMO. However, SE and EE are two trade-off criteria, so generally one tends to increase and the other to decrease. In Fig. 3, SE-EE values (green curves) calculated according to all values of number of the users and number of the antennas are shown. The red curve is true Pareto optimal front (true POF) which consisted by all non-dominated solutions. A non-dominated solution means that there is no solution has higher SE and EE value on the solution set.

When Fig. 3 is examined, it is seen that all curves are non-convex and non-concave type, so SE-EE trade-off cannot be formulated in a simple way. Although determining the Pareto curve after calculating SE and EE values for all cases provides a solution to the problem, this process is quite lengthy. Instead, determining the input parameters by optimization and finding examples of ideal solutions or values very close to these are considered as a reasonable option. In this paper, this option has been implemented by using multi-objective bat algorithm.

Intelligent optimization techniques are fast, flexible and successful techniques whose use is increasing day by day. Thanks to these techniques, populations that develop

themselves in every iteration are used without making calculations for all probabilities of variable parameters. Through these optimizations, samples can be obtained from ideal results or very close to ideal results with much less calculations.

In this paper, multi-objective bat algorithm (MOBA) has been used on SE-EE trade-off and it has been compared with multi-objective genetic algorithm (MOGA), multi-objective differential evolution algorithm (MODEA) and multi-objective particle swarm optimization (MOPSO).

### 3 Multi-objective bat algorithm

Multi-objective bat algorithm (MOBA) was inspired by the echolocation behaviour of microbats. Microbats use a type of sonar, called, echolocation, to detect prey, avoid obstacles. These bats emit a very loud sound pulse and listen for the echo that bounces back from the surrounding objects. Their pulses can be correlated with their hunting strategies, depending on the species. Studies show that microbats use the time delay from the emission and detection of the echo, the time difference between their two ears, and the loudness variations of the echoes to build up three-dimensional scenario of the surrounding [14].

MOBA contains parameters called loudness and pulse emission rate which are adapted from behaviour of microbats. These parameters effect to randomization ratios of updating of population. These rates start with the value of 0.9 and decrease as the iterations continue. This situation causes the possibility of modification to new solutions increases, and the probability of random position assignment to population members decreases considerably as

$$A^{t+1} = \alpha A^t, \quad (1)$$

$$r^t = r^0 [1 - \exp(-\gamma t)], \quad (2)$$

where  $A^t$  is loudness at iteration number  $t$ ,  $r^t$  is rate of pulse emission at iteration number  $t$ ,  $\alpha$  and  $\gamma$  are constants.

The algorithm updates entire population at each iteration. New positions are produced in two stages by taking advantage of the position of the best population. Pseudo code of MOBA applied to SE-EE trade-off problem is given in Fig. 4.

In the optimizations used in the simulations, necessary changes and additions have been made on the standard MOBA. The modifications of search steps of the optimization parameters ( $K, M, p$ ) are key modifications. It is also critical to change the algorithm to optimize over integers.

### 4 Simulation results

The stages in the simulations are creating sample cells, calculating SE for all combinations of independent variables, calculating EE for the same combinations, and finally finding sample non-dominated SE-EE values with

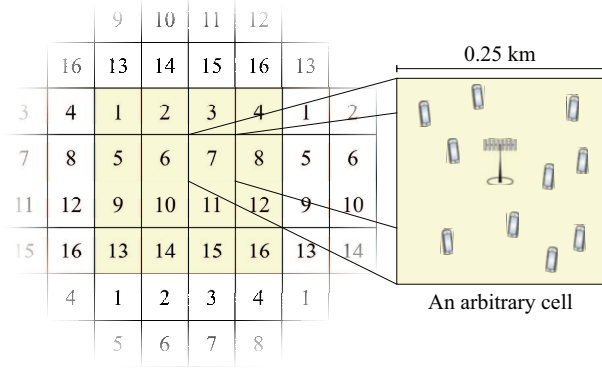


Fig. 5. Illustration of cell layouts and an arbitrary cell [1]

an intelligent optimization method. Calculation of SE and EE values is represented as

$$[S, \mathcal{E}] = \text{Calculate}(K, M, p). \quad (3)$$

where  $S(K, M, p)$  stands for SE, while  $\mathcal{E}(K, M, p)$  stands for EE. The number of users served among the cell ( $K$ ), the number of active antennas in the cell ( $M$ ) and the transmission power ( $p$ ), are the independent variables. While  $K$  and  $M$  parameters take integer values between 10 and 100,  $p$  takes values between 50 and 200 mW

The parameters of the sample created cells for use in simulations are given in Tab. 1.

Table 1. Simulation parameters

| Parameter                          | Value                        |
|------------------------------------|------------------------------|
| Network layout                     | Square pattern (wrap-around) |
| Number of cells ( $L$ )            | 16                           |
| Cell area                          | 0.25 km $\times$ 0.25 km     |
| Channel gain at 1 km               | $\gamma = -148.1$ dB         |
| Pathloss exponent                  | $\alpha = 3.76$              |
| Shadow fading (standard deviation) | $\sigma_{sf} = 10$           |
| Bandwidth ( $B$ )                  | 20 MHz                       |
| Receiver noise power               | -94 dBm                      |
| Samples per coherence block        | $\tau_c = 200$               |
| Pilot reuse factor                 | $f = 1$                      |

As seen in Fig. 5, each cell's edges are in the form of a square area of 250 meters in length. Users are randomly distributed into these cells at a distance of at least 35 meters from other users and the base station (BS). After the cells are created, spatial correlation matrices ( $R$ ) are created in the dimensions of the number of users and the number of antennas. The channels are selected as correlated Rayleigh fading and the average channel gains of all transmission channels are calculated accordingly. Afterwards, channel realization and channel estimation of all channels are made. Calculation of spectral efficiency ( $S$ ) for coding and decoding algorithms is performed according to

$$S_j = \sum_{k=1}^{K_j} (mS_{jk}^{\text{UL}} + n \max(\underline{S}_{jk}^{\text{DL}}, S_{jk}^{\text{DL}})), \quad (4)$$

by summing in certain proportion the SE for uplink denoted as  $S^{\text{UL}}$ , and SE for downlink, denoted  $S^{\text{DL}}$ . In this paper, it was chosen;  $m = 1/3$  and  $n = 2/3$ . Further,  $j$  is the number of cell and  $k$  is the number of UE and  $\underline{S}^{\text{DL}}$  represents hardening bound of SE for DL and  $S^{\text{DL}}$  represents estimation bound of SE for DL. While the UL spectral efficiency is based on detecting the information signal with a linear acquisition combination, the DL SE calculation is based on choosing the larger of the hardening bound and the estimation bound.

Detailed calculation of SE is shown below

$$S_{jk}^{\text{UL}} = \frac{\tau_u}{\tau_c} E\{\log_2(1 + Z_{jk}^{\text{UL}})\}, \quad (5)$$

$$Z_{jk}^{\text{UL}} = \frac{p_{jk} |v_{jk}^H \hat{h}_{jk}^j|^2}{\sum_{l=1}^L \sum_{\substack{i=1 \\ (l,i) \neq (j,k)}}^{K_l} p_{li} |v_{jk}^H \hat{h}_{li}^j|^2 + v_{jk}^H \left( \sum_{l=1}^L \sum_{i=1}^{K_l} p_{li} C_{li}^j + \sigma_{\text{UL}}^2 I_{M_j} \right) v_{jk}}, \quad (6)$$

$$\underline{S}_{jk}^{\text{DL}} = \frac{\tau_d}{\tau_c} \log_2(1 + \underline{Z}_{jk}^{\text{DL}}), \quad (7)$$

$$\underline{Z}_{jk}^{\text{DL}} = \frac{\rho_{jk} |E\{w_{jk}^H h_{jk}^j\}|^2}{\sum_{l=1}^L \sum_{i=1}^{K_l} \rho_{li} E\{|w_{li}^H h_{li}^j|^2\} - \rho_{jk} |E\{w_{jk}^H h_{jk}^j\}|^2 + \sigma_{DL}^2}, \quad (8)$$

$$S_{jk}^{\text{DL}} = \frac{\tau_d}{\tau_c} E\{\log_2(1 + Z_{jk}^{\text{DL}})\} - \sum_{i=1}^{K_j} \frac{1}{\tau_c} \log_2 \left( 1 + \frac{\rho_{ji} \tau_d V\{w_{ji}^H h_{jk}^j\}}{\sigma_{DL}^2} \right), \quad (9)$$

$$Z_{jk}^{\text{DL}} = \frac{\rho_{jk} |w_{jk}^H h_{jk}^j|^2}{\sum_{\substack{i=1 \\ i \neq k}}^{K_j} \rho_{ji} |w_{ji}^H h_{jk}^j|^2 + \sum_{\substack{l=1 \\ l \neq j}}^{K_l} \sum_{i=1}^{K_l} \rho_{li} E\{|w_{li}^H h_{jk}^j|^2\} + \sigma_{DL}^2}. \quad (10)$$

Here  $\tau_u$  is UL data samples per coherence block,  $\tau_c$  is the number of samples per coherence block,  $E\{\}$  is expectation of a random variable,  $Z$  stands for signal-to-interference-and-noise-ratio (in abbreviation SINR),  $p$  is UL transmit power,  $v$  is receive combining vector,  $\hat{h}$  is estimate of the channel,  $C$  is estimation error correlation matrix for channel,  $\sigma^2$  is noise variance,  $I_M$  is  $M \times M$

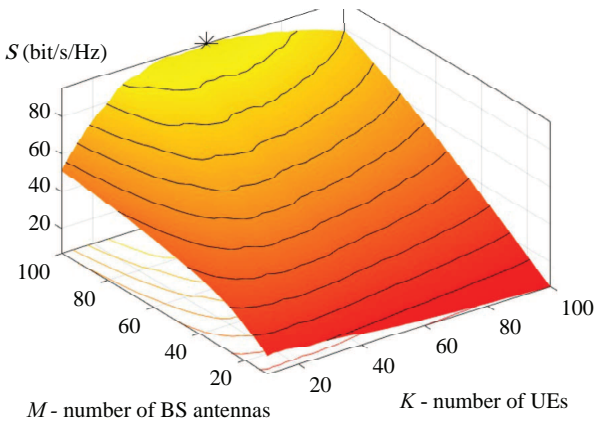


Fig. 6. SE at different K and M values

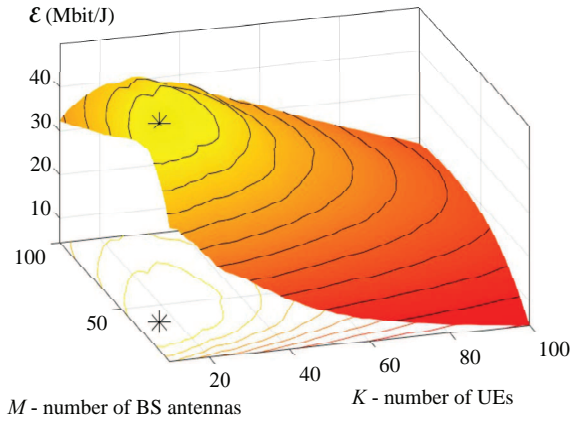


Fig. 7. EE at different K and M values

identity matrix,  $\tau_d$  is DL data samples per coherence block,  $\rho$  is DL transmit power,  $w$  is transmit precoding vector,  $h$  is channel response and  $V$  is variance of a random variable, respectively.

When Fig. 6 is examined, in case the transmission power is 50 mW, the SE values are shown as a function of parameters  $S(K, N)$ . It is seen that the maximum  $S$  value is at point  $(K, M) = (56, 100)$ , that is the highest possible antenna number.

The study was aimed to calculate the EE value or  $\mathcal{E}(M, K)$  for the input combination with SE found as  $S(M, K)$ , then SE is calculated as in [1].

$$\mathcal{E}_j = \frac{S_j B}{P_j^{\text{TE}} + P_j^{\text{C}}} \quad (11)$$

where  $B$  is the bandwidth,  $P_j^{\text{TE}}$  is effective transmit power and  $P_j^{\text{C}}$  is the consumed power, not used in the transmission.

Figure 7 shows found EE values  $\mathcal{E}$  when the transmission power is 50 mW and the highest EE value is seen at the relatively small  $(K, M) = (16, 38)$  point.

SE-EE calculations are made for all combinations of input parameters and then true Pareto front is determined. This process, which takes quite a long time, is carried out to be a reference to the optimization results. After this process is completed, the non-dominated ones are determined from the results obtained by applying the optimization processes sequentially, each optimization with a population of 100 elements and makes 50 iterations. The calculation results of all values of the parameters whose effects are examined are shown with green curves and true Pareto front with red curve, while non-dominated values determined by intelligent optimization algorithms are shown with black asterisks.

It is seen from Fig. 8 that MOGA did not success to perform successfully on the problem. It has found several solutions on the true Pareto, but other solutions it finds are far from the Pareto curve. If both the number of iterations and the population size increase, success may increase. Some power parameters used in EE calculations are given in Tab. 2.

Table 2. Power parameters

| Parameter                                      | Value            |
|--|------------------|
| Fixed power: $P_{\text{FIX}}$                  | 5 W              |
| Power for BS local oscillator: $P_{\text{LO}}$ | 0.1 W            |
| Power per BS antennas: $P_{\text{BS}}$         | 0.2 W            |
| Power per UE: $P_{\text{UE}}$                  | 0.1 W            |
| Power for data encoding: $P_{\text{COD}}$      | 0.03 W/(Gbit/s)  |
| Power for data decoding: $P_{\text{DEC}}$      | 0.24 W/(Gbit/s)  |
| BS computational efficiency: $L_{\text{BS}}$   | 225 Gflops/W     |
| Power for backhaul traffic: $P_{\text{BT}}$    | 0.075 W/(Gbit/s) |

It is seen from Fig. 9 that most of the non-dominated solutions obtained with MODEA have been on or very close to the true Pareto curve. However, it is seen that these solutions are not good enough distributed in all regions and they are concentrated in regions where SE is high.

When the MOPSO results are examined in Fig. 10, it has showed a more balanced distribution than MODEA, and the solutions, with a few exceptions, are on Pareto curve or very close to the curve. However, no solution has been found in the bigger than 95.3 SE region and so this algorithm's inverted generational distance term is very high.

From Fig. 11 it is seen that there are results in both the maximum SE and maximum EE regions and their surroundings, and the majority of the results found are close to the true Pareto front. As a result, it can be said that the performance of MOBA is high.

Performance metrics of each algorithm are given in Tab. 3 for comparison. These metrics are inverted generational distance (IGD), maximum spread (MS) and spacing metric (SM). IGD shows the total Euclidean distance between estimated Pareto curve and the true Pareto front

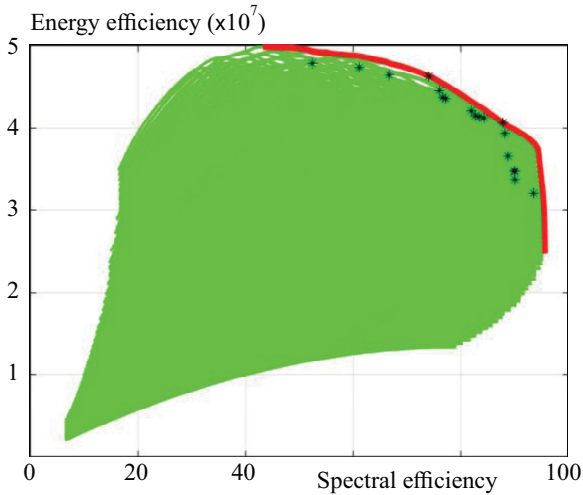


Fig. 8. Comparing true POF and performance of MOGA on SE-EE trade-off

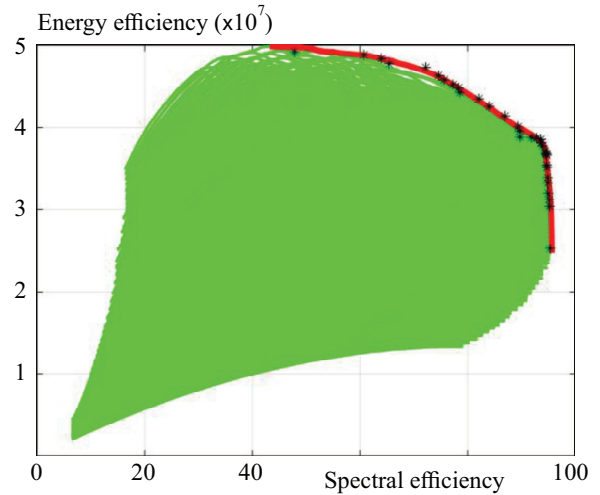


Fig. 9. Comparing true POF and performance of MODEA on SE-EE trade-off

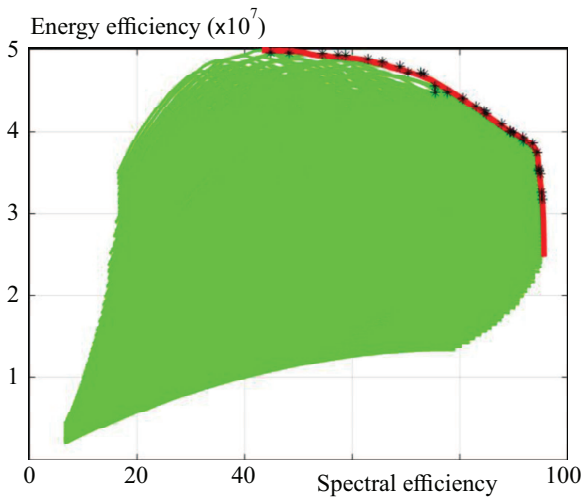


Fig. 10. Comparing true POF and performance of MOPSO on SE-EE trade-off

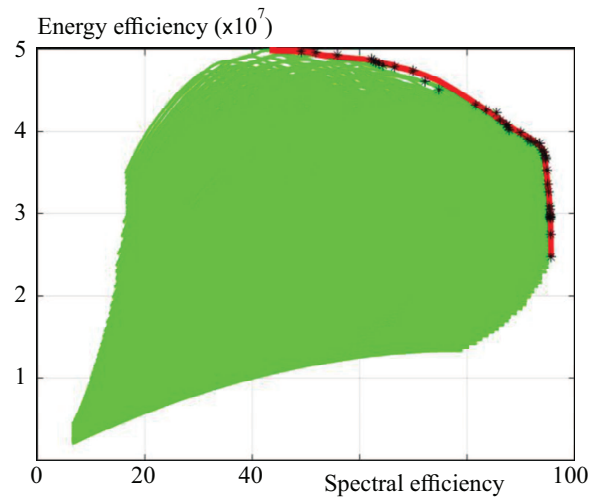


Fig. 11. Comparing true POF and performance of MOBA on SE-EE trade-off

Table 3. Comparison of the performance metric of the algorithms.

| Algorithm  | IGD                | MS    | SM                 |
|------------|--------------------|-------|--------------------|
| MOGA [18]  | $1.51 \times 10^6$ | 0.712 | $0.87 \times 10^6$ |
| MODEA [19] | $0.42 \times 10^6$ | 0.929 | $1.31 \times 10^6$ |
| MOPSO [20] | $1.13 \times 10^6$ | 0.845 | $0.59 \times 10^6$ |
| MOBA       | $0.26 \times 10^6$ | 0.942 | $0.84 \times 10^6$ |

[15]. The low value of this term indicates that the solutions are successful. MS indicates the amount of overlap between the estimated Pareto curve and the true Pareto front [16]. The high level of this term means that the success of the algorithm about this subject is high. SM refers to the distance between the found values and con-

secutive ones [17]. The lowness of this parameter means that the distribution of the values found is of good quality. When the performance metrics are examined, it is seen that MOBA is the best algorithm in IGD and MS terms and the second-best algorithm in SM term.

Figure 12 shows the variations of the number of non-dominated solutions according to the number of iterations for used intelligent optimization algorithms. According to Fig. 12, MOBA finds 42 different non-dominated solutions whereas MODEA finds 33 different non-dominated solutions, MOPSO finds 31 different non-dominated solutions and MOGA finds 19 different non-dominated solutions. Having more non-dominated solutions is an important criterion as it improves the quality of overlap with true POF. If the number of samples on the Pareto curve reaches a sufficient level, the Pareto curve estimation can be achieved.

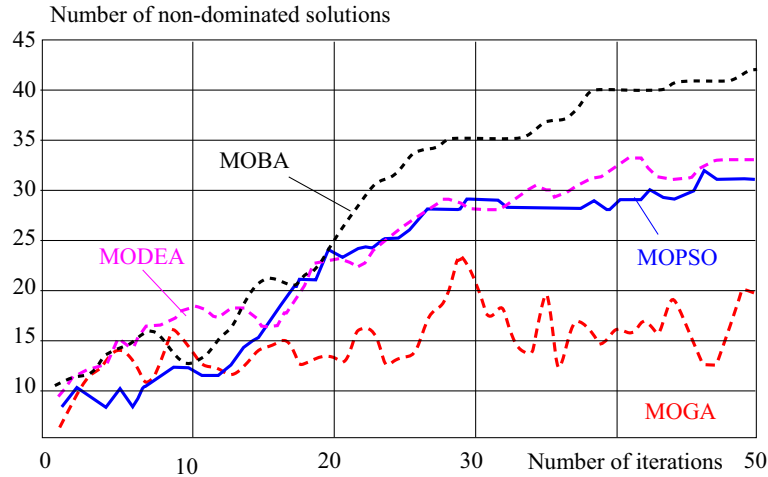


Fig. 12. The variations of the numbers of non-dominated solutions versus the number of iterations for algorithms used in simulations

## 5 Conclusion

It is seen that, thanks to intelligent optimizations, it is possible to determine a reasonably similar set of results to the Pareto curve without calculating for all probabilities of the independent variables. Although the solutions found with optimizations are at a level that cannot exactly create the real Pareto curve, they have drastically reduced the time to reach the solution. When the algorithms used in simulations are compared with each other, it can be said that MOBA has the best performance. It is considered that reaching a high number of non-dominated solutions in a shorter time than other algorithms contributed to this success.

## REFERENCES

- [1] E. Björnson, J. Hoydis, and L. Sanguinetti, "Massive MIMO Networks: Spectral, Energy and Hardware Efficiency", *Foundation and Trends in Signal Processing*, pp. 154–655, doi: 10.1561/20000000093, 2017.
- [2] A. Fehske, G. Fettweis, J. Malmolin, and G. Biczok, "The Global Footprint of Mobile Communications: The Ecological and Economic Perspective", *IEEE Transactions on Wireless Communications* vol. 49, no. 8, pp. 55–62, doi: 10.1109/MCOM.2011.5978416, 2011.
- [3] Q. He, L. Xiao, X. Zhong, and S. Zhou, "Increasing the Sum-throughput of Cells with a Sectorization Method for Massive MIMO", *IEEE Communications Letters*, vol. 18, no. 10, pp. 1827–1830, doi: 10.1109/LCOMM.2014.2346483, 2014.
- [4] B. Zhang, Y. Tian, and W. Wang, "On the Downlink Throughput Capacity of Hybrid Wireless Networks with Massive MIMO", *Eurasip Journal on Wireless Communications and Networking*, vol. 1, no. 110, pp. 26086–26091, doi: 10.1186/s13638-018-1134-1, 2018.
- [5] G. Yang, C. K. Ho, R. Zhang, and Y. L. Guan, "Throughput Optimization for Massive MIMO Systems Powered by Wireless Energy Transfer", *IEEE Journal on Selected Areas in Communications* vol. 33, no. 8, pp. 1640–1650, doi: 10.1109/JSAC.2015.2391835, 2015.
- [6] F. Heydari, S. Ghazi-Maghrebi, A. Shahzadi, and M. J. R. Fatemi, "Better spectral efficiency of device to device underlying massive multi-input multi-output using receiver filter algorithm and power control model", *International Journal of Communication Systems*, vol. 34, no. 5, pp. e4655, doi: 10.1002/dac.4655, 2021.
- [7] T. Zeng, and E. Ouyang, "Massive multi-in multi-out multiuser multiplexing based on transmission mode 3", *International Journal of Communication Systems*, vol. 34, no. 7, pp. e4761, doi: 10.1002/dac.4761, 2021.
- [8] A. Shukla, V. Goyal, M. Kumar, M. C. Trivedi, and V. K. Deolia, "MMSE based beamformer in massive MIMO-IDMA downlink systems", *Journal of Electrical Engineering*, vol. 71, no. 1, pp. 65–68, doi: 10.2478/jee-2020-0010, 2020.
- [9] B. K. Gül, and N. Taşpınar, "Application of Intelligent Optimization Techniques to Spectral and Energy Efficiencies in Massive MIMO Systems at Different Circuit Power Levels", *Mühendislik Bilimleri ve Arastirmalari Dergisi*, vol. 3, no. 1, pp. 102–111, doi: 10.46387/bjesr.893643, 2021.
- [10] Z. Liu, W. Du, and D. Sun, "Energy and Spectral Efficiency Tradeoff for Massive MIMO Systems with Transmit Antenna Selection", *IEEE Transactions on Vehicular Technology*, vol. 66, no. 5, pp. 4453–4457, doi: 10.1109/TVT.2016.2598842, 2017.
- [11] Y. Hei, C. Zhang, W. Song, and Y. Kou, "Energy and Spectral Efficiency Tradeoff in Massive MIMO Systems with Multi-objective Adaptive Genetic Algorithm", *Soft Computing*, vol. 23, no. 16, pp. 7163–7179, doi: 10.1007/s00500-018-3356-x, 2019.
- [12] E. Björnson, E. G. Larsson, and M. Debbah, "Massive MIMO for Maximal Spectral Efficiency: How Many Users and Pilots Should Be Allocated?", *IEEE Transactions on Wireless Communications*, vol. 15, no. 2, pp. 1293–1308, doi: 10.1109/TWC.2015.2488634, 2015.
- [13] L. Li, W. Meng, and S. Ju, "A novel artificial bee colony detection algorithm for massive MIMO system", *Wireless Communications and Mobile Computing*, vol. 16, pp. 3139–3152, doi: 10.1002/wcm.2754, 2016.
- [14] X.-S. Yang, "Bat algorithm for multi-objective optimisation", *International Journal of Bio-Inspired Computation*, vol. 3, no. 4, pp. 267–274, doi: 10.1504/IJBIC.2011.042259, 2011.
- [15] Y. Yuan, H. Xu, B. Zhang, and X. Yao, "Balancing convergence and diversity in decomposition-based many-objective optimizers", *IEEE Transactions on Evolutionary Computation*, vol. 19, no. 5, pp. 694–716, doi: 10.1109/TEVC.2015.2443001, 2015.
- [16] C. Goh, and K. C. Tan, "An investigation on noisy environments in evolutionary multiobjective optimization", *IEEE Transactions on Evolutionary Computation*, vol. 11, no. 3, pp. 354–381, doi: 10.1109/TEVC.2006.882428, 2007.

- [17] J. Schott, "Fault tolerant design using single and multicriteria genetic algorithm optimization", *MS thesis, Massachusetts Technology*, 1995.
- [18] T. Murata, and H. Ishibuchi, "MOGA: Multiobjective genetic algorithms", *Proc. of IEEE International Conference on Evolutionary Computation*, pp. 289–294, 1995.
- [19] W. Gong, and Z. Cai, "A multiobjective differential evolution algorithm for constrained optimization", *IEEE Congress on Evolutionary Computation*, pp. 181–188, doi: 10.1109/CEC.2008.4630796, 2008.
- [20] C. A. C. Coello, G. T. Pulido, and M. S. Lechuga, "Handling multiple objectives with particle swarm optimization", *IEEE Transactions on Evolutionary Computation*, vol. 8, no. 3, pp. 256–279, doi: 10.1109/TEVC.2004.826067, 2004.

Received 19 January 2022

**Burak Kürşat Gül** received his degree of BS in Electronics Engineering from Uludag University, Bursa, Turkey in 2012, and MS degree in Electrical and Electronics Engineering from Ondokuz Mayıs University, Samsun, Turkey in 2017. He has been studying PhD in Electrical and Electronics Engineering at Erciyes University, Kayseri, Turkey since 2017,

and he has been a Research Assistant since 2013. His research interests include massive MIMO systems and intelligent optimization methods.

**Necmi Taşpınar** received the BS degree in Electronics Engineering from Erciyes University, Kayseri, Turkey in 1983, the MS degree in Electronics and Telecommunications Engineering from Technical University of Istanbul, Istanbul, Turkey in 1988, and the PhD degree in Electronics Engineering from Erciyes University, Kayseri, Turkey in 1991. From 1984 to 2002, he worked as Research Assistant, Assistant Professor and Associate Professor at Erciyes University, Kayseri, Turkey. Since 2002 he has been Full Professor in the Department of Electrical and Electronics Engineering, Erciyes University, Kayseri, Turkey. His research interests include ARQ schemes, multi-user detection, channel estimation, pilot tones design, PAPR reduction methods, CDMA systems, MC-CDMA systems, OFDM systems, MIMO systems, IDMA systems, massive MIMO systems, optics communications and applications of neural networks and intelligent optimization methods to communication problems.

---